

# Axial Mode Helical Antennas

HISAMATSU NAKANO, MEMBER, IEEE, YUJI SAMADA, AND JUNJI YAMAUCHI, MEMBER, IEEE

**Abstract**—The radiation characteristics of helical antennas operating in the axial mode are evaluated on the basis of the theoretical current distributions and are verified by experimental work. A comparison between monofilar helix and bifilar helix antennas is made, and a helical antenna with a parasitic helix (HAP) is proposed in order to enhance the power gain. It is found that the gain of the HAP in which the parasitic helix is wound from a point diametrically opposite to that of one and one-half turns of the driven helix is about 1 dB higher than that of the monofilar helix. The ratio of the frequency band in which the HAP radiates a circularly polarized wave within an axial ratio of 3 dB is calculated to be 1:1.8.

## INTRODUCTION

AN AXIAL MODE helical antenna has been used as a circularly polarized radiator with a wide bandwidth. The fundamental information for designing this antenna is given by Kraus [1], who has derived an approximate expression for the gain on the basis of a large number of experimental radiation patterns. King and Wong [2] have also presented the gain characteristics of the axial mode helical antenna with its turns ranging from five to 35. Their experimental research reveals the gain slope as a function of frequency and the peak gain as a function of the number of turns, together with radiation patterns. Recently, Lee and Wong evaluated the gain, assuming the current along the helix to be a single outward traveling wave of constant amplitude [3]. They discussed the discrepancy between the gain values obtained from the formula given by Kraus and the measurements made by King and Wong.

It is well known that we can enhance the power gain by increasing the number of helical turns, properly choosing the helical circumference. This method, however, forces us to expand the antenna length unreasonably. The purpose of this paper is to explore the possibilities of increasing the power gain with the axial length remaining unchanged.

First, attention is paid to a comparison between a monofilar helical antenna [4]–[9] and a bifilar helical antenna [10]. On the basis of the theoretical current distributions, the radiation fields are evaluated, and the power gain of the bifilar helix is found to be higher than that of the monofilar helix. However, the bifilar helix has the disadvantage of a complicated feeding system, since the two inputs have to be excited with antiphase relation.

Because the current distribution of the axial mode monofilar helix is divided into a decaying wave region and a surface

wave region [11], [12], we propose a helical antenna with a parasitic helix which is wound only on the surface wave region of the driven helix. Detailed studies show how the current distribution and the power gain are affected by the location of the parasitic helix (HAP). It is demonstrated that the proposed helix can realize an enhanced gain, while maintaining a simple feeding system. The ratio of the frequency band in which the proposed helix has an axial ratio of less than 3 dB is found to be 1:1.8.

## MONOFILAR AND BIFILAR HELICAL ANTENNAS

A previous study [11] has numerically revealed that the current distribution of a monofilar helix operating in the axial mode is composed of two distinct regions. One is a region  $C$  where the current decays smoothly from the input to the minimum. The other is a surface wave region  $S$  where the current has nearly constant amplitude and approximately satisfies the in-phase condition for the endfire radiation. To be more exact, the phase velocity in the region  $S$  does not exceed that of the in-phase condition.

Fig. 1(a) shows the configuration and the coordinate system of a monofilar helical antenna to be used as a reference antenna in the following discussions. The number of helical turns  $n_d$  is eight; the pitch angle  $\alpha$  is  $12.5^\circ$ ; the circumference of the helical cylinder  $C_h$  is 10 cm, which corresponds to one wavelength ( $1\lambda$ ) at a frequency of 3 GHz; the wire radius  $\rho$  is 0.5 mm. The helical wire of two turns near the open end is tapered to reduce the reflected current with consequent improvement in the axial ratio [5], [13]. In the present analysis the antenna is treated as a helix mounted on an infinite ground plane allowing the use of the image theory, i.e., as a balanced type helix, and is fed by a delta-function generator of 1 V.

The radiation pattern (electric fields of  $E_\theta$  and  $E_\phi$ ), which is calculated from the theoretical current distribution of Fig. 1(b), is illustrated in Fig. 1(c) together with the experimental data. It should be noted that the theoretical current distribution is obtained using an integral equation [5]. Since the radiation patterns at each azimuth are similar to each other, it is shown for only one principal plane. The average half-power beamwidth (HPBW) of  $E_\theta$  and  $E_\phi$  components at  $\phi = 90^\circ$  plane is about  $52^\circ$ , and the maximum sidelobe level is about  $-8$  dB. The axial ratio indicates an excellent value of 0.7 dB (experimental value was 0.8 dB) on the helical axis. The power gain is calculated to be 10.6 dB from

$$G(\theta, \phi) = \frac{[|E_\theta|^2 + |E_\phi|^2]r_0^2}{30|I(0)|^2R_l} \quad (1)$$

where  $I(0)$  is the theoretical current at the antenna input,  $R_l$  is

Manuscript received September 17, 1985; revised March 29, 1986.  
H. Nakano and Y. Samada are with the College of Engineering, Hosei University, 3-7-2 Kajino-cho, Koganei, Tokyo 184, Japan.  
J. Yamauchi is with Tokyo Metropolitan Technical College, 1-10-40 Higashi-Ooi, Shinagawa-ku, Tokyo, 140 Japan.  
IEEE Log Number 8609135.

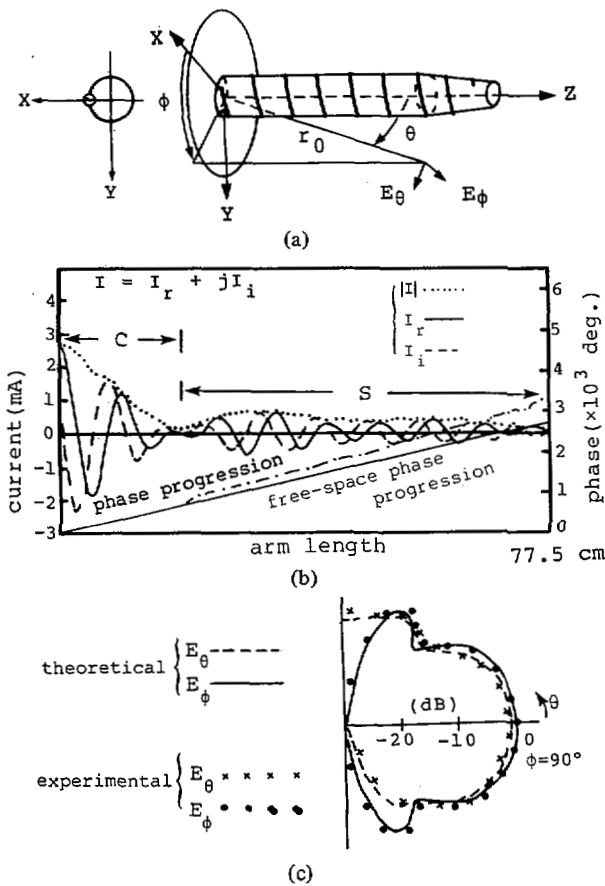


Fig. 1. (a) Configuration and coordinate system. (b) Current distribution. (c) Radiation pattern of a monofilar helical antenna. The number of helical turns  $n_d =$  eight, pitch angle  $\alpha = 12.5^\circ$ , circumference of helical cylinder  $C_h = 10$  cm, wire radius  $\rho = 0.5$  mm, and frequency  $f = 3$  GHz.

the resistance of the antenna input impedance ( $= 0.5 V/I(0)$  A), and  $r_0$  is the distance from the origin to a field point as shown in Fig. 1(a).

Now consider enhancing the power gain. The most well-known means is to increase the number of helical turns  $n_d$  with subsequent increase in the axial length. The behavior of the theoretical power gain of the monofilar helix is shown in Fig. 2, as a function of the axial length. It is noted that the power gain is close to the experimental result by King and Wong [2], although the present antenna backed by an infinite ground plane reflector has the configuration parameters different from those of their antenna backed by a cavity. The difference in the gain shown in Fig. 2 is about 0.5 dB. The slightly lower value in the computed gain is partially due to the employment of the two-turn end taper. Fig. 2 also shows that the power gain in the present antenna increases, for instance, from 10.6 dB to 13.1 dB as the  $n_d$  is increased from eight to 16. This simple means of increasing the power gain by the helical turns, however, forces us to unreasonably expand the axial length of the antenna from  $1.7 \lambda$  to  $3.5 \lambda$  (from 17.2 cm to 34.9 cm at 3 GHz).

The increased power gain can also be realized by adding another helical wire or by a bifilar helical antenna [10], as shown in Fig. 3(a). The two helical wires with the same pitch angle are wound from two points diametrically opposite to

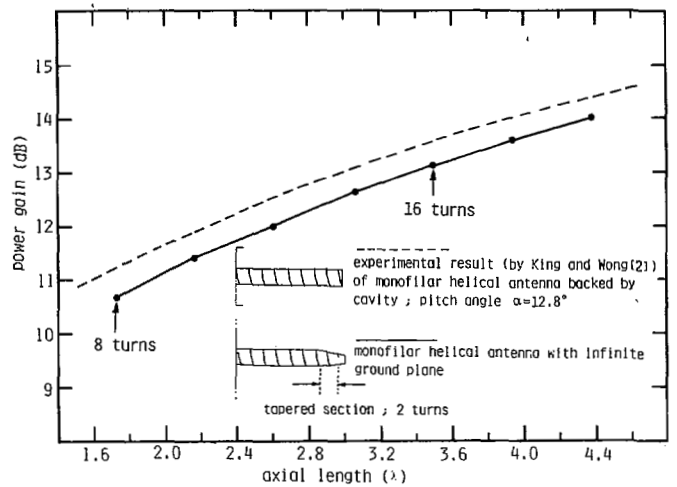


Fig. 2. The theoretical power gain of a monofilar helical antenna as a function of the axial length. The circumference of helical cylinder  $C_h$  is  $1 \lambda$ .

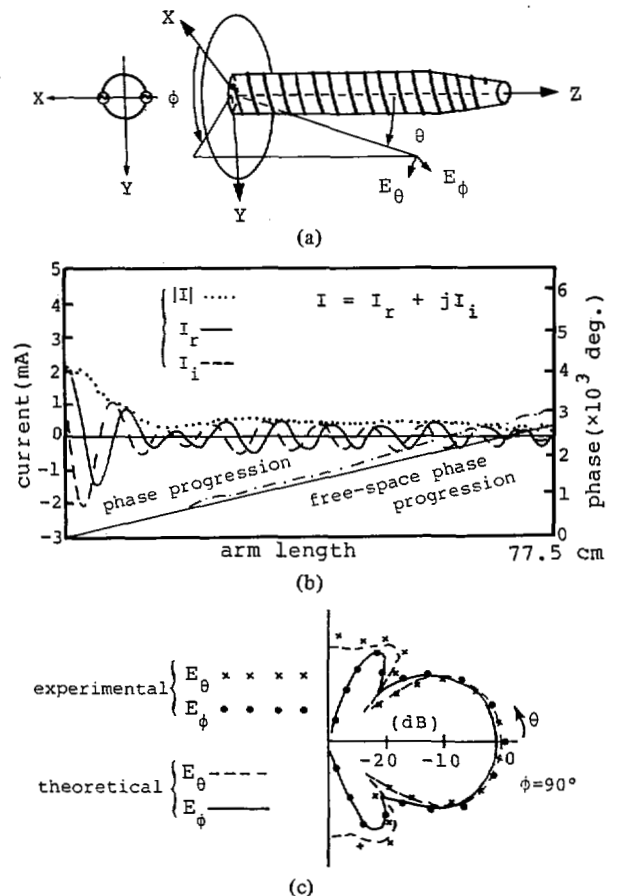


Fig. 3. (a) Configuration and coordinate system. (b) Current distribution. (c) Radiation pattern of a bifilar helical antenna. The number of helical turns  $n_d =$  eight, pitch angle  $\alpha = 12.5^\circ$ , circumference  $C_h = 10$  cm, wire radius  $\rho = 0.5$  mm, and frequency  $f = 3$  GHz.

each other, and the two inputs are excited with antiphase relation.

The theoretical current distribution of the bifilar helix is shown in Fig. 3(b), where the number of helical turns  $n_d$ , the pitch angle  $\alpha$  and the wire radius are the same as those used in Fig. 1(a);  $n_d =$  eight,  $\alpha = 12.5^\circ$  and  $\rho = 0.5$  mm. Since the currents on the two wires are the same in the amplitude, only

the current on the one wire is presented. The form of the current distribution is found to be similar to that observed in the monofilar helix in that the two distinct regions *C* and *S* appear.

Examination of the radiation pattern shown in Fig. 3(c) reveals that the main beam is narrower than that of the monofilar helix shown in Fig. 1(c). The half-power beamwidth (HPBW) of the bifilar helix is 44°, while that of the monofilar helix is 52°. Consequently, an increased power gain of 12.3 dB is obtained in the bifilar helix. This value is determined from (1) in which the coefficient of 30 in the denominator is changed to 60 because of the bifilar helix, and is 1.7 dB higher than the power gain of the monofilar helix. It is worth mentioning that the increased power gain is realized with the axial length remaining unchanged.

From the above-mentioned results, it can be said that a means of winding two helical wires and exciting the two inputs with antiphase relation is effective in enhancing the power gain. However, we are forced to use a hybrid circuit to excite the two inputs with antiphase relation.

### HELICAL ANTENNA WITH A PARASITIC HELIX

It is interesting to consider the case where one wire of a bifilar helix is not excited, i.e., used as a parasite whose input terminal is open, since the current must be induced on the parasitic helix due to the mutual coupling between the driven and parasitic helices. Fig. 4(b) shows the theoretical current distribution of Fig. 4(a) in which the one wire of the bifilar helix shown in Fig. 3(a) is not excited. The standing wave is noticeable on the driven and parasitic helices. The form of the current distribution is markedly different from those of the monofilar helix in Fig. 1(b) and the bifilar helix in Fig. 3(b).

Fig. 4(c) is the radiation pattern evaluated using the current distribution shown in Fig. 4(b). From the radiation pattern the power gain is calculated to be 12.1 dB, which is close to that of the bifilar helix shown in Fig. 3(a). It should be noted, however, that the input impedance does not keep constant over a wide range of frequencies, as shown in Fig. 4(d). Since the variation of the input impedance is caused by the standing wave distribution of the current, it is necessary to realize a traveling wave distribution of the current on both the driven and parasitic helices.

It should be recalled that the current distribution of a monofilar helix operating in the axial mode is divided into two regions *C* and *S*. Because the decaying wave region *C* acts as an exciter and the surface wave region *S* as a director, we reach an idea that a parasitic helix should be wound only on the cylinder where the driven helix establishes a surface wave region. We designate this type of helical antenna as a HAP (see Fig. 5(a)).

Fig. 5(b) shows the current distribution on a HAP composed of the driven helix with the helical turns of  $n_d =$  eight, which is the same as the monofilar helix shown in Fig. 1(a), and the parasitic helix with the helical turns of  $n_p =$  six. The latter is wound from a point diametrically opposite to that of two turns of the driven helix. It is found that the form of the decaying wave region on the driven helix remains unchanged despite adding the parasitic helix. The decaying wave region again

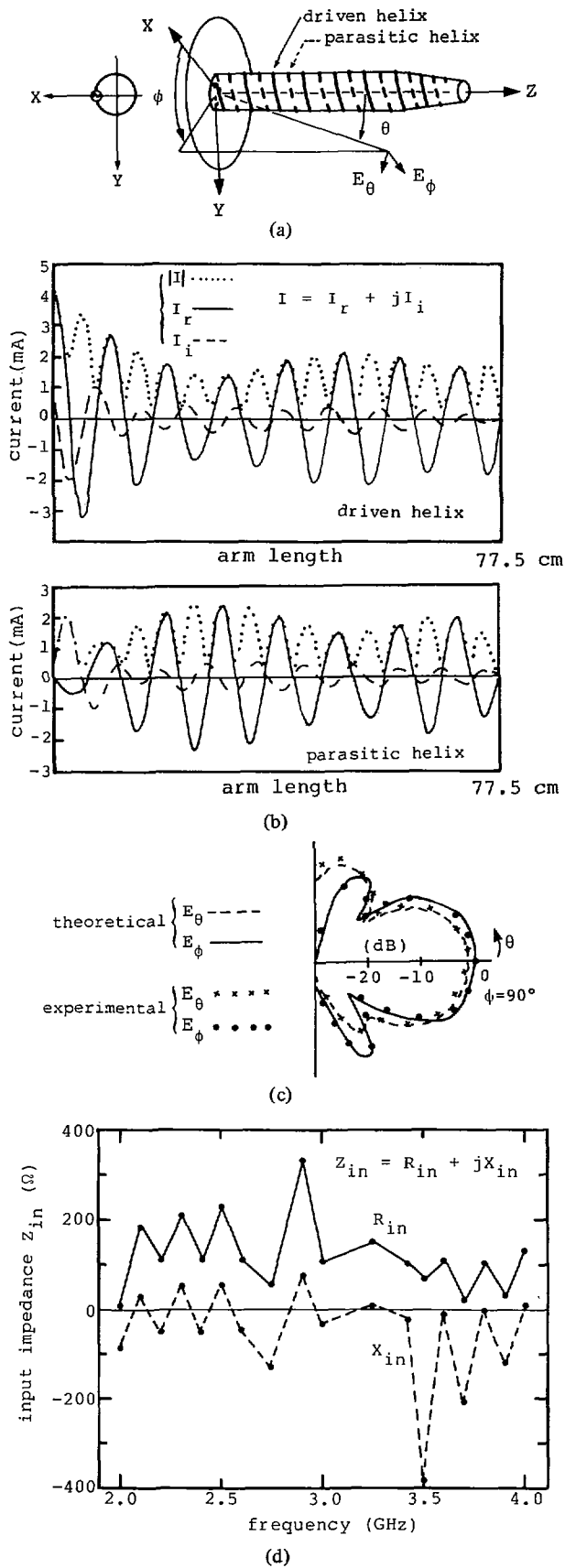


Fig. 4. (a) Configuration and coordinate system. (b) Current distribution. (c) Radiation pattern at 3 GHz. (d) Frequency characteristic of the input impedance of a bifilar helical antenna where the one arm is not excited. The number of helical turns  $n_d =$  eight, pitch angle  $\alpha = 12.5^\circ$ , circumference  $C_h = 10$  cm, wire radius  $\rho = 0.5$  mm.

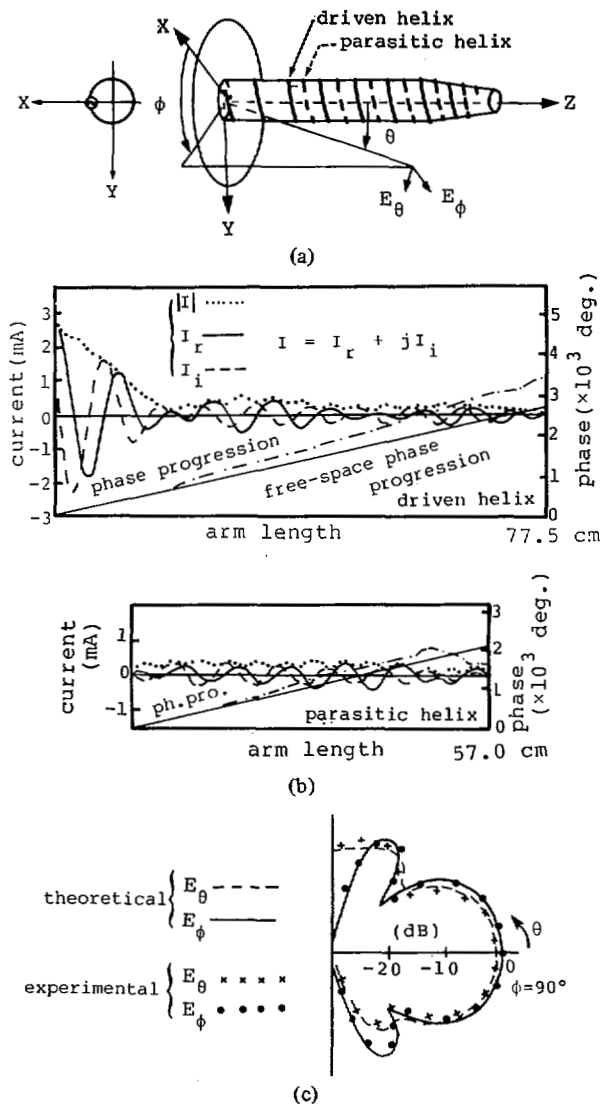


Fig. 5. (a) Configuration and coordinate system. (b) Current distribution. (c) Radiation pattern of a helical antenna with a parasitic helix. The number of driven helical turns  $n_d =$  eight, the number of parasitic helical turns  $n_p =$  six, pitch angle  $\alpha = 12.5^\circ$ , circumference  $C_h = 10$  cm, wire radius  $\rho = 0.5$  mm, and frequency  $f = 3$  GHz.

acts as an exciter for the remaining turns of both the driven and parasitic helices. The remaining turns of each helix have the current of relatively constant amplitude and act as a director.

The relative phase velocity is defined as the ratio of the phase velocity of the current on the wire to the light velocity. Both the relative phase velocities of the currents of the driven and parasitic helices on the surface wave region are almost the same as a value of 0.82 of the monofilar helix shown in Fig. 1(a). In addition, the sum of the current amplitude in the surface wave region on the driven helix and that on the parasitic helix is larger than the amplitude on the monofilar helix.

Fig. 5(c) illustrates the radiation pattern. The HPBW is calculated to be  $47^\circ$ , which is narrower than that of the monofilar helix shown in Fig. 1(c). An increased power gain of 11.4 dB not obtainable in the monofilar helix is realized. Although the power gain of 11.4 dB is somewhat lower than 12.3 dB obtained in the bifilar helix shown in Fig. 3(a), it

should be noted that the use of a parasitic helix contributes to the enhancement of the power gain with an advantage of a single feed of the antenna.

The enhancement of the gain can be explained as follows. The denominator in (1) remains unchanged despite of adding the parasitic helix, since the current value at the input of the HAP is nearly the same as that of the monofilar helix. This means that the higher gain is caused by the increase in the numerator, or the electric field. Since the current in the surface wave region approximately satisfies the in-phase condition for the endfire radiation, the increase in the current amplitude leads to the increase in the electric field in the direction of the Z-axis. It should be recalled that the sum of the current amplitude in the surface wave region on the driven helix and that on the parasitic helix is larger than the amplitude on the monofilar helix. Consequently, the gain is enhanced by the addition of the parasitic helix.

#### LOCATION OF A PARASITIC HELIX

In the previous section, a prototype of a helical antenna with a parasitic helix on an infinite ground plane or a HAP has been made at a single frequency where the circumference of the helical cylinder corresponds to one wavelength. In practical application, it is desirable to keep an increased gain over a wide range of frequencies.

The fundamental concept for designing the HAP is that the parasitic helix should be wound only over the surface wave region of the driven helix in order to establish a traveling wave distribution of the current. Hence it is important to choose the location of a starting point of the winding of the parasitic helix.

In this section two types of HAP's are investigated from the standpoint of frequency characteristics. One is a HAP in which a parasitic helix is wound from a point diametrically opposite to that of one and one-half turns of the driven helix of  $n_d =$  eight turns. The other is wound from a point of two turns, which is identical to the HAP shown in Fig. 5(a). The two HAP's are designated as type (A) and type (B), respectively. It should be noted that the type (A) is made on the basis of the shift of the minimum in the current distribution. The end point of the region C or the minimum point of the current distribution shifts slightly toward the feed point as the frequency is increased. As shown in Fig. 6, the minimum point at 3.7 GHz is located near a point of one and one-half turns.

Fig. 7 shows the frequency characteristics of the power gains and the axial ratios of two types of HAP's. For comparison those of the monofilar helix shown in Fig. 1(a) are also given by the lines labeled as M. It should be emphasized that the gain of type (A) is about 1 dB higher than that of the monofilar helix, and that the bandwidth of type (A) is wider than that of type (B). The increase in the gain of type (A) is explained by the fact that it has the desirable current distribution which is dominated by a traveling wave of a nearly in-phase condition for the endfire radiation over a wide range of frequencies, as shown in Fig. 8(a). On the other hand, as indicated in Fig. 8(b), type (B) shows standing wave behavior in the current distribution at higher frequencies, with subsequent narrowness of the bandwidth.

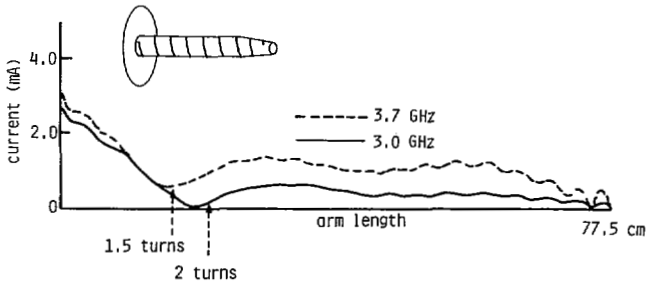


Fig. 6. Frequency characteristic of the current distribution of a monofilar helical antenna. The number of helical turns  $n_d =$  eight, pitch angle  $\alpha = 12.5^\circ$ , circumference  $C_h = 10$  cm, and wire radius  $\rho = 0.5$  mm.

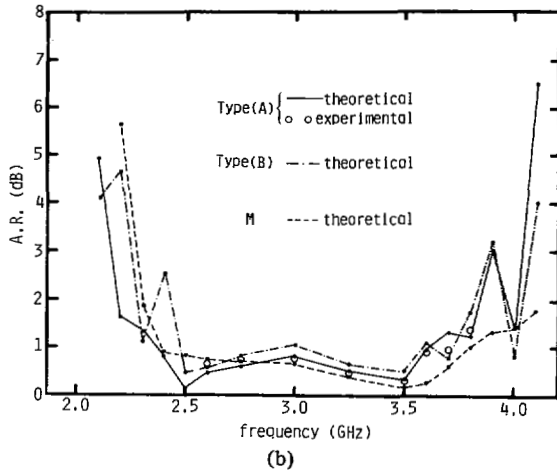
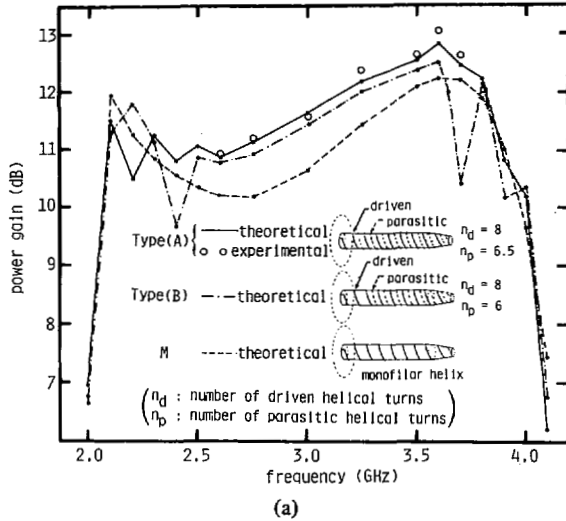


Fig. 7. Frequency characteristics. (a) Power gains. (b) Axial ratios of type (A) and type (B). Pitch angle  $\alpha = 12.5^\circ$ , circumference  $C_h = 10$  cm, and wire radius  $\rho = 0.5$  mm.

In summary, it can be said that type (A) has a good choice of the location for the starting point of the winding of the parasitic helix and realizes a higher power gain over a frequency range of 1:1.8, where the axial ratio remains within 3 dB, having the advantage of a single feed. For further reference, the input impedance characteristics of type (A) and the monofilar helix are shown in Fig. 9. The input impedance of type (A) is on the order of  $160 \pm 60$  ohms in the resistive value and  $-70 \pm 35$  ohms in the reactive value over the above-mentioned frequency range.

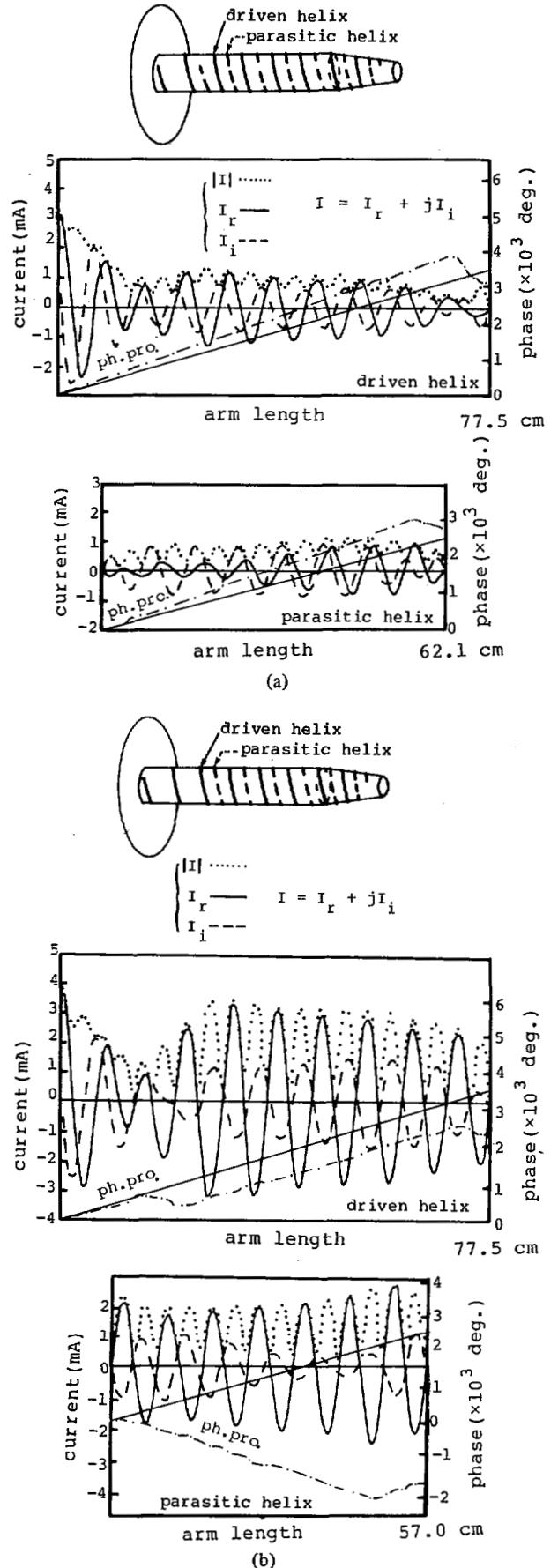


Fig. 8. (a) Current distribution of type (A). (b) Current distribution of type (B). Both are at 3.7 GHz.

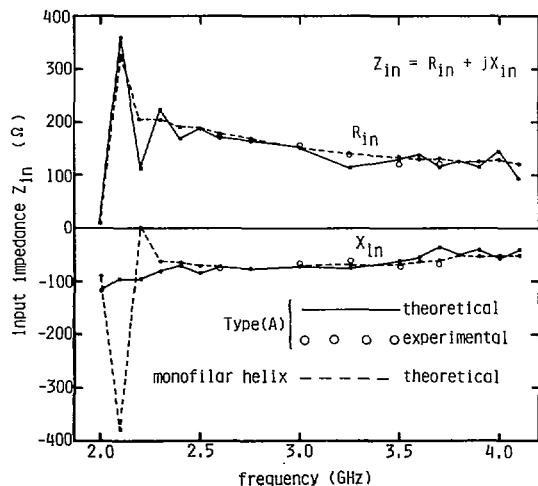


Fig. 9. Frequency characteristics of the input impedance of type (A) and a monofilar helical antenna.

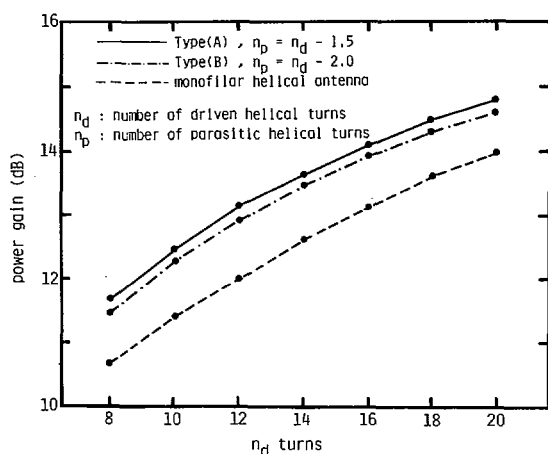


Fig. 10. Power gains as a function of the number of helical turns. Pitch angle  $\alpha = 12.5^\circ$ , circumference  $C_h = 10$  cm, wire radius  $\rho = 0.5$  mm, and frequency  $f = 3$  GHz.

So far we have referred to the three antennas of type (A), type (B), and monofilar helix, fixing the number of the driven helix turns  $n_d$  to be eight. The power gains when the number of the driven helix turns is changed are shown in Fig. 10. It is found that type (A) is about 1 dB higher than that of the monofilar helix at any number of the driven helix turns.

### CONCLUSION

The radiation characteristics of axial mode helical antennas have been calculated using the theoretical current distributions. Although a bifilar helix has a higher gain than a monofilar helix, it requires a complicated feeding system with a hybrid circuit. To eliminate the complexity and maintain an increased power gain, a helical antenna with a parasitic helix has been proposed and discussed.

Since the parasitic helix should be wound on a surface wave region of the driven helix, special attention is paid to the

location of a starting point of the winding of the parasitic helix. It is found that the gain of a HAP in which the parasitic helix is wound from a point diametrically opposite to that of one and one-half turns of the driven helix is about 1 dB higher than that of the monofilar helix. The ratio of the frequency band in which the HAP radiates a circularly polarized wave within an axial ratio of 3 dB is calculated to be 1:1.8.

### ACKNOWLEDGMENT

We would like to express our indebtedness to Mr. H. Mimaki for his kind assistance in arranging the data in this paper.

### REFERENCES

- [1] J. D. Kraus, *Antennas*. New York: McGraw-Hill, 1947.
- [2] H. E. King and J. L. Wong, "Characteristics of 1 to 8 wavelength uniform helical antennas," *IEEE Trans. Antennas Propagat.*, vol. AP-28, pp. 291-296, 1980.
- [3] K. F. Lee and P. F. Wong, "Directivities of helical antennas radiating in the axial mode," *Proc. Inst. Elec. Eng.*, pt. H, vol. 131, pp. 121-122, 1984.
- [4] R. C. Johnson and H. Jasik, Ed., *Antenna Engineering Handbook*. New York: McGraw-Hill, 1984, ch. 13.
- [5] H. Nakano and J. Yamauchi, "Characteristics of modified spiral and helical antennas," *Proc. Inst. Elec. Eng.*, pt. H, vol. 129, pp. 232-237, 1982.
- [6] H. Nakano, J. Yamauchi, H. Mimaki, and M. Sugano, "The balanced helical antenna radiating right- and left-hand circularly-polarized-waves," *IECE Japan*, vol. 63-B, pp. 743-750, 1980.
- [7] T. Shiokawa and Y. Karasawa, "Radiation characteristics of axial-mode helical antenna," *IECE Japan*, vol. 63-B, pp. 143-150, 1980.
- [8] K. F. Lee, P. F. Wong, and K. F. Larm, "Theory of the frequency responses of uniform and quasi-taper helical antennas," *IEEE Trans. Antennas Propagat.*, vol. AP-30, pp. 1017-1021, 1982.
- [9] R. G. Vaughan and J. B. Andersen, "Polarization properties of the axial mode helix antenna," *IEEE Trans. Antennas Propagat.*, vol. AP-33, pp. 10-20, 1985.
- [10] A. G. Holtum, "Improving the helical beam antennas," *Electron.*, vol. 29, pp. 99-101, 1960.
- [11] H. Nakano and J. Yamauchi, "Radiation characteristics of helix antenna with parasitic elements," *Electron. Lett.*, vol. 16, pp. 687-688, 1980.
- [12] H. Nakano, T. Yamane, and J. Yamauchi, "Directive properties of parasitic helix and its application to circularly polarised antenna," *Proc. Inst. Elec. Eng.*, pt. H, vol. 130, pp. 391-396, 1983.
- [13] D. J. Angelakos and D. Kajfez, "Modifications of the axial-mode helical antenna," *Proc. IEEE*, vol. 55, pp. 558-559, 1967.

Hisamatsu Nakano (M'75), for a photograph and biography please see page 840 of the August 1984 issue of this TRANSACTIONS.



Yuji Samada was born in Mie, Japan, on September 22, 1961. He received the B.E. and M.E. degrees in electrical engineering from Hosei University, Japan, in 1984 and 1986, respectively.

He joined the Sony Co. Ltd., Tokyo, in 1986. Mr. Samada is a member of the Institute of Electronics and Communication Engineers of Japan.

Junji Yamauchi (M'84), for a photograph and biography please see page 840 of the August 1984 issue of this TRANSACTIONS.